

## COB-2023-2248

# ANALYSIS OF THE DYNAMICS AND ENERGY EFFICIENCY OF A NONIDEAL PORTAL FRAME STRUCTURAL SUPPORT SYSTEM COUPLED TO A PASSIVE ABSORBER

**Angelo M. Tusset**

**Jose Manoel Balthazar**

Federal University of Technology – Paraná (UTFPR), R. Doutor Washington Subtil Chueire, 330 - Jardim Carvalho, Ponta Grossa - PR, 84017-220. Brazil.

a.m.tusset@gmail.com; jmbaltha@gmail.com

**Abstract.** *In this work, a dynamic analysis of an energy collector model is presented, based on a simple gantry structure, considered a non-ideal excitation system, and the coupling of an NES system as a source of energy absorption. Energy harvesting is performed using piezoelectric material coupled to the gantry structure. The dynamic analysis of the system is performed considering, time history, phase diagrams, and the 0-1 test. Numerical simulations, considering variation of the coupling parameters of the piezoelectric material and the NES absorber are presented. The simulation results demonstrate that for certain system parameters, chaotic, quasi-periodic and periodic behavior is observed. Variations of the average energy harvesting power for parametric variations are also observed. With the obtained results it was possible to demonstrate that the use of the passive absorber makes it possible to suppress the chaotic behavior of the system, as well as to increase the energy generation, being only necessary to adjust the mass, rigidity and damping of the absorber.*

**Keywords:** *nonlinear dynamics, nonlinear systems, nonideal systems, energy harvesting, nonlinear energy sink*

## 1. INTRODUCTION

Recently, there has been much interest in the concepts of electro-mechanical systems that are able to scavenge, or harvest energy from their operating environment. As the kinetic energy is a source of energy easily found in the environment, devices that convert kinetic energy into electrical energy have been widely studied, and special attention has been devoted to devices that use piezoelectric elements as a means of energy transduction. Research about non-ideal problems also have been increased considerably in technical-scientific community.

Nonlinear problems have been widely studied due to their particularities in real problems, mainly when these nonlinearities induce interactions between a dynamical system with its excitation source, these kinds of systems are called non-ideal systems. One of the excitation sources, which is of non-ideal kind, is an unbalanced DC motor with limited power supply.

Energy harvesting is one of the most promising sources currently, contributing significantly to clean energy generation, considering the capture of wasted or unused energy in the environment. Usually captured from wind sources, photovoltaic steam flow, or using piezoelectric materials that transform vibration into energy. The main advantage of capturing energy using piezoelectric materials is that it does not depend on climatic and environmental conditions, such as solar, wind and thermal energy. Since the piezoelectric collectors are installed in places frequently subject to mechanical and vibrational efforts, such as bridges or highways (Pan et al., 2021; Aoudia et al., 2018; Selleri et al. 2023; Lai et al., 2019).

Energy harvesting from vibrational sources has the advantages of its configuration, output power and electromechanical conversion efficiency. Since their discovery, piezoelectric materials have been applied in advanced technologies in several areas, such as energy harvesting, given their ability to sense and collect vibrations (Koga et al., 2017; Shi et al., 2018; Eiras et al., 2016; Vallem et al., 2021).

The capture of energy through piezoelectric materials has shown to be a solution to the challenges of producing clean energy since it allows the transforming of environmental energy sources into electrical energy, energy normally wasted (Shaukat et al., 2023).

This potential for obtaining energy has attracted the attention of many researchers, seeking to obtain energy from different vibrational sources, such as collecting energy from the oceans (Du et al., 2022), wind (Lu et al., 2022), rain (Bao et al., 2021) and road vibration (Ye et al., 2023).

Energy harvesting by piezoelectric materials has applications in areas such as health and biomedicine (Mokhtari et al., 2021; Wu et al., 2021), wireless data transmission (Liew et al., 2023; Panayanthatta et al., 2021; Dinesh et al., 2022),

aeronautics (Tommasino et al., 2023; Elahi et al., 2020; Holzmann et al., 2021), environmental monitoring and artificial intelligence (Cao et al., 2021), among others.

In this context, this work investigates the application of materials with piezoelectric characteristics for micro-energy generation, considering a U-type gantry system coupled to a motor in continuous operation and a nonlinear energy dissipator (NES), acting as a passive vibration absorber.

## 2. MATHEMATICAL MODEL

Figure 1 shows the structure of the system investigated in this work, the system consisting of a U-shaped gantry structure base with non-linear rigidity, and a non-linear energy sink (NES), with the piezoelectric material attached to the side of the structure.

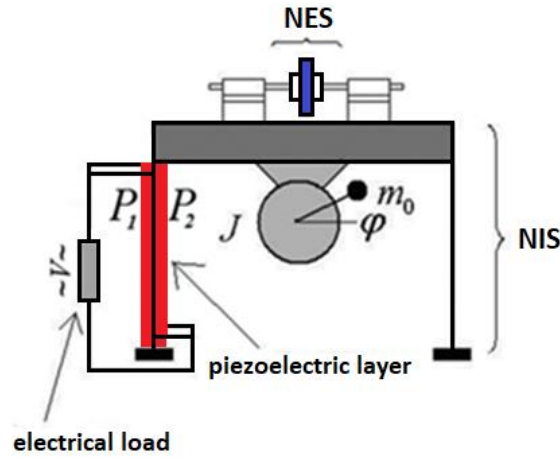


Figure 1. U-shaped portal frame structure with non-linear energy sink and coupled piezoelectric material.

Figure 2 presents the physical model of the system represented in figure 1.

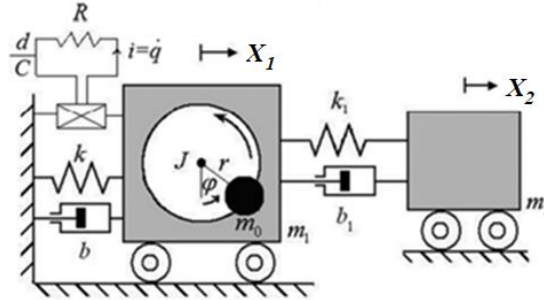


Figure 2. Physical model of the U-frame structure with non-linear energy sink and coupled piezoelectric material.

The equation of motion of the electromechanical system represented by figure 2 is given by the following equation (Iliuk et al., 2014):

$$\begin{aligned}
 (m_1 + m_0)\ddot{X}_1 + b\dot{X}_1 + b_1(\dot{X}_1 - \dot{X}_2) - k_l X_1 + k_{nl} X_1^3 + k_1(X_1 - X_2)^3 \\
 = m_0 r (\ddot{\varphi} \sin(\varphi) + \dot{\varphi}^2 \cos(\varphi)) + \frac{d(X_1)}{C} q \\
 m_2 \ddot{X}_2 - b_1(\dot{X}_1 - \dot{X}_2) - k_1(X_1 - X_2)^3 = 0 \\
 (J + r^2 m_0) \ddot{\varphi} - r m_0 \ddot{X}_1 \sin(\varphi) = V_1 - V_2 \dot{\varphi} \\
 R \dot{q} - \frac{d(X_1)}{C} X_1 + \frac{q}{C} = 0
 \end{aligned} \tag{1}$$

According to Iliuk et al., (2014), the electrical charge developed in the coupled circuit is given by  $q$ , and the term  $\frac{d(X_1)}{c} q$  represents the piezoelectric coupling to the mechanical component, with a strain-dependent coupling coefficient  $d(x)$ .

The system represented by equation 1 can be rewritten in dimensionless form considering the following substitutions (Iliuk et al., 2014):

$$\tau = \omega_1 t, \quad x = \frac{rX_1}{\omega_1^2}, \quad z = \frac{rX_2}{\omega_1^2}, \quad \omega_1 = \sqrt{\frac{k_l}{(m_1+m_0)}}, \quad \alpha_1 = \frac{b}{(m_1+m_0)\omega_1}, \quad \beta_1 = \frac{k_l}{(m_1+m_0)\omega_1^2}, \quad \beta_3 = \frac{k_{nl}r^2}{(m_1+m_0)\omega_1^6}, \quad \delta_1 = \frac{m_0\omega_1^2}{(m_1+m_0)}, \quad \rho_1 = \frac{m_0r^2}{(J+r^2m_0)\omega_1^2}, \quad \rho_2 = \frac{V_1}{(J+r^2m_0)\omega_1^2}, \quad \rho_3 = \frac{V_2}{(J+r^2m_0)\omega_1}, \quad \alpha_2 = \frac{b_1}{m_2\omega_1}, \quad \alpha_3 = \frac{k_1r^2}{m_1}, \quad \varepsilon_1 = \frac{m_1b_1}{m_2\omega_1}, \quad \varepsilon_2 = k_1r^2, \quad v = \frac{q}{q_0}, \quad \rho = \frac{RC}{\omega_1} \text{ and } d(X_1) = \theta(1 + \theta|x|).$$

Considering the substitutions above, system 1 can be represented in the following dimensionless form:

$$\begin{aligned} \ddot{x} - \beta_1 x + \alpha \dot{x} + \alpha_2(\dot{x} - \dot{z}) + \beta_3 x^3 + \alpha_3(x - z)^3 - \theta(1 + \theta|x|)v &= \delta_1 \ddot{\varphi} \sin \varphi + \delta_1 \dot{\varphi}^2 \cos \varphi \\ \ddot{z} - \varepsilon_1(\dot{x} - \dot{z}) - \varepsilon_2(x - z)^3 &= 0 \\ \ddot{\varphi} &= \rho_1 \cos \varphi \ddot{x} - \rho_3 \dot{\varphi} + \rho_2 \\ \rho \dot{v} - \theta(1 + \theta|x|)x + v &= 0 \end{aligned} \quad (2)$$

Using new variables defined as:  $x_1 = x$ ,  $x_2 = \dot{x}$ ,  $x_3 = z$ ,  $x_4 = \dot{z}$ ,  $x_5 = \varphi$ ,  $x_6 = \dot{\varphi}$  and  $x_7 = v$ , the equations may be rewritten in state space representation as:

$$\begin{aligned} \dot{x}_1 &= x_2 \\ \dot{x}_2 &= \frac{1}{\Delta} \left( \beta_1 x_1 - \alpha_1 x_2 - \alpha_2(x_2 - x_4) - \beta_3 x_1^3 - \alpha_3(x_1 - x_3)^3 + \right. \\ &\quad \left. + \theta(1 + \theta|x_1|)x_7 + \delta_1 \cos(x_5)x_6^2 + \delta_1 \sin(x_5)(-\rho_3 x_6 + \rho_2) \right) \\ \dot{x}_3 &= x_4 \\ \dot{x}_4 &= \varepsilon_1(x_2 - x_4) + \varepsilon_2(x_1 - x_3)^3 \\ \dot{x}_5 &= x_6 \\ \dot{x}_6 &= \frac{1}{\Delta} \left( -\rho_3 x_6 + \rho_2 + \rho_1 \cos(x_5)(\beta_1 x_1 - \alpha_1 x_2 - \alpha_2(x_2 - x_4) - \beta_3 x_1^3 - \right. \\ &\quad \left. - \alpha_3(x_1 - x_3)^3 + \theta(1 + \theta|x_1|)x_7 + \delta_1 \cos(x_5)x_6^2 \right) \\ \dot{x}_7 &= (\theta(1 + \theta|x_1|)x_1 - x_7)/\rho \end{aligned} \quad (3)$$

where  $\Delta = 1 - \rho_1 \cos(x_5)\delta_1 \sin(x_5)$ .

The average power is obtained through (Iliuk et al., 2014):

$$P_{avg} = \frac{1}{T} \int_0^T P(\tau) d\tau \quad (4)$$

Where instantaneous power is calculated using the following:

$$P = \rho \dot{x}_7^2 \quad (5)$$

For analysis of the periodic or chaotic behavior of the system, the 0-1 test proposed by Gottwald and Melbourne (2004, 2005) is considered, consisting of estimating a parameter  $K$ .

Acord to Litak et al. (2013) and Bernardini and Litak (2016) for  $K$  value close to 0, the system is periodic, and if the  $K$  value is close to 1, the system is chaotic.

### 3. NUMERICAL RESULTS

For numerical simulations, Eq. (3) was considered, integrated by the 4<sup>th</sup> order Runge-Kutta method, with integration step ( $h=0.01$ ), with fixed parameters:  $\alpha_1 = 0.1$ ,  $\alpha_2 = 0.1$ ,  $\alpha_3 = 0.5$ ,  $\beta_1 = 1$ ,  $\beta_3 = 0.2$ ,  $\delta_1 = 8.373$ ,  $\rho_1 = 0.05$ ,  $\rho_2 = 100$ ,  $\rho_3 = 200$ ,  $\varepsilon_1 = 1$ ,  $\varepsilon_2 = 5$ ,  $\theta = 0.20$ ,  $\theta = 0.60$  and  $\rho = 1$  (Iliuk et al., 2014). And variation in parameters  $\varepsilon_1 = [0.01: 2]$ ,  $\varepsilon_2 = [1: 10]$  and  $\rho = [0.01: 2]$ .

The calculation of the average power will be obtained through equation 4. The behavior analysis is performed by analyzing the variations of  $K$  from test 0-1, according to equation 9. This paper will consider chaotic behavior for the system when  $K \geq 0.8$ , undefined behavior when  $0.3 \leq K \leq 0.79$ , and periodic behavior when  $K < 0.3$ .

Figure 3 presents the  $K$  variations of the 0-1 test and the variations of the average power setting the parameter  $\rho = 1.0$ , and considering  $\varepsilon_1 = [0.01: 2]$  versus  $\varepsilon_2 = [1: 10]$ .

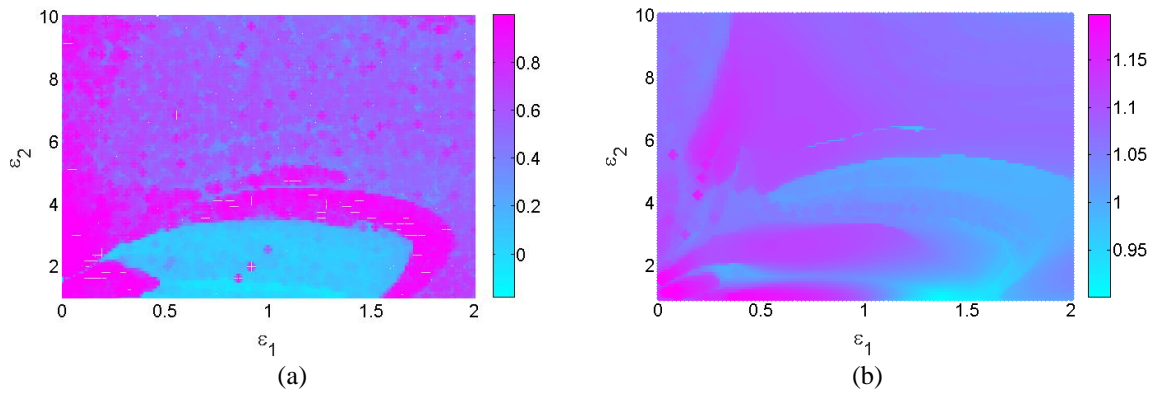


Figure 3. Variation in parameters  $\varepsilon_1 = [0.01: 2]$  versus  $\varepsilon_2 = [1: 10]$ . (a) Test 0-1. (b) Average Power.

According to the results presented in figure 3b, the greatest potential for energy generation is obtained when parameters close to  $\varepsilon_1 = 0.0502$  and  $\varepsilon_2 = 1.182$  are considered, providing an average power estimate  $P_{avg} \approx 1.198$ .

It can also be observed in figure 3a that, for these parameters, the lateral displacements become chaotic with the value of  $K \approx 0.9$ .

However, analyzing the results of figure 3, it is observed that for  $\varepsilon_1 = 0.3919$  and  $\varepsilon_2 = 1$  there is also a potential for energy generation in regions of maximums, with an estimated average power of  $P_{avg} \approx 1.184$ . However, in this case, the lateral displacements have a periodic behavior, with  $K \approx 0$ .

Figure 4 shows the phase diagram of the gantry and the NES as well as the time history of the electrical voltage generated by the piezoelectric material for the parameters:  $\varepsilon_1 = 0.0502$  and  $\varepsilon_2 = 1.182$ . And in Figure 5 for parameters:  $\varepsilon_1 = 0.3919$  and  $\varepsilon_2 = 1$ .

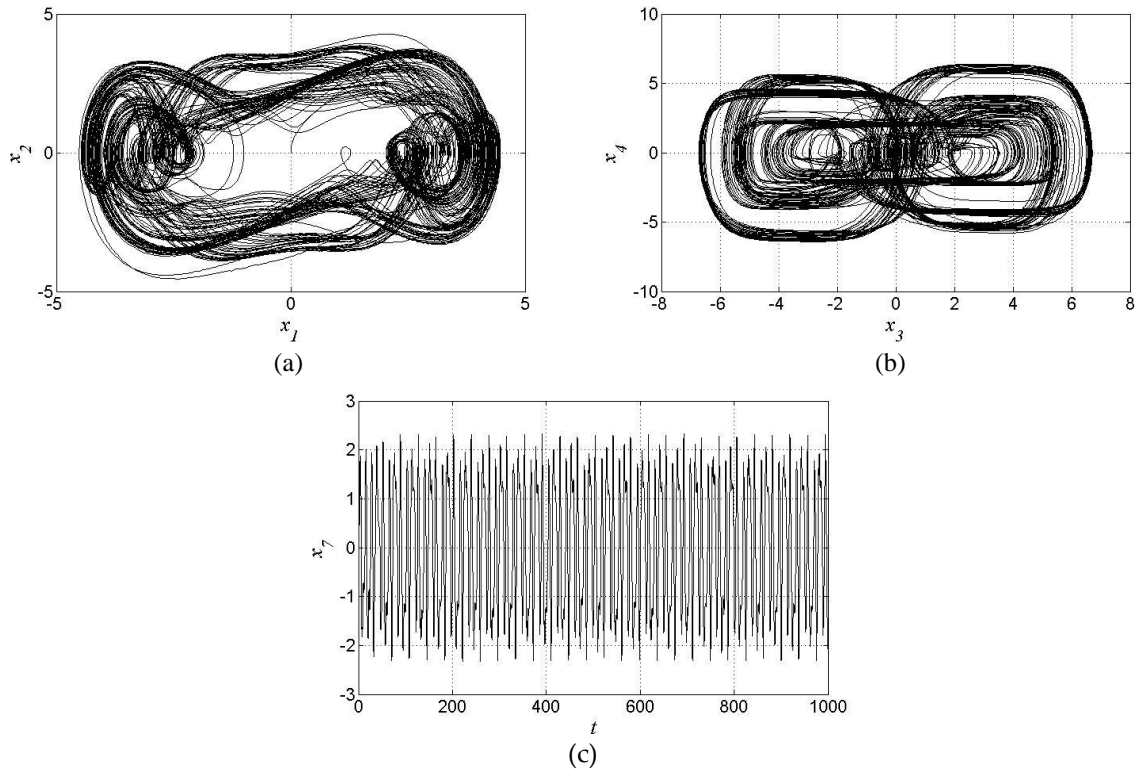


Figure 4. Case that  $\varepsilon_1 = 0.0502$  and  $\varepsilon_2 = 1.182$ . (a) Phase diagram  $x_1$  versus  $x_2$ . (b) Phase diagram  $x_1$  versus  $x_2$ . (c) Variation of electrical voltage.

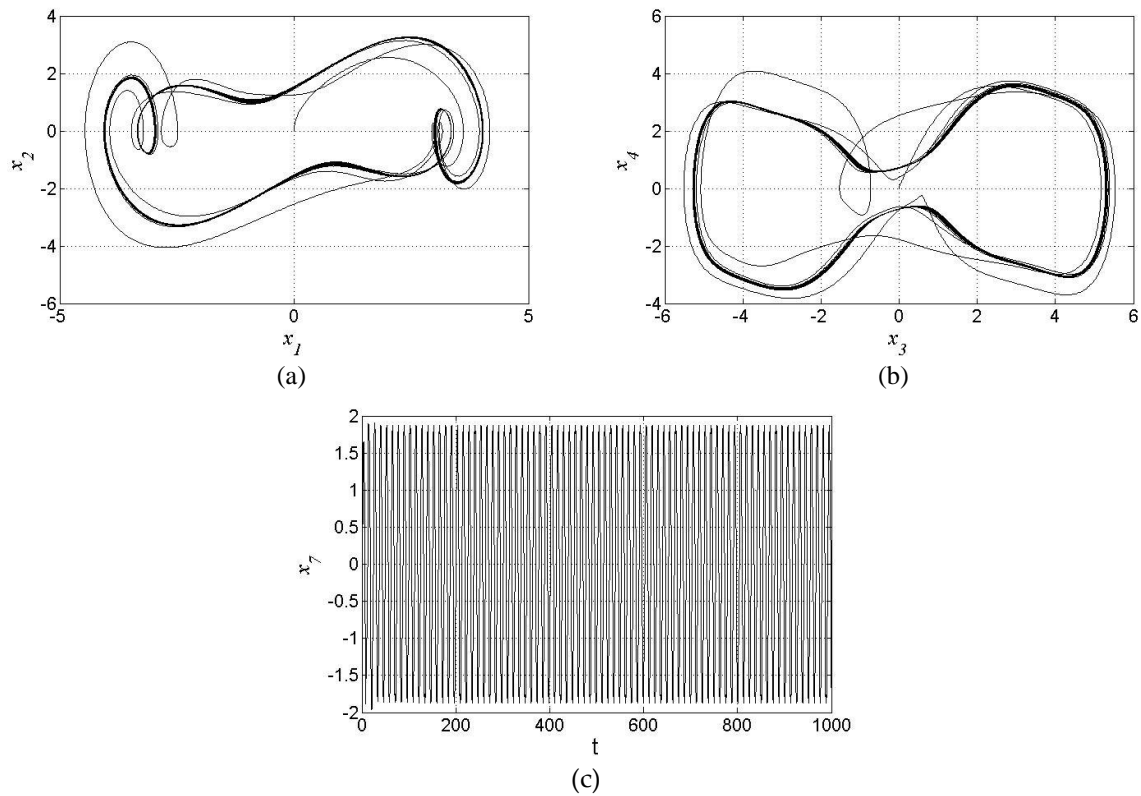


Figure 5. Case that  $\varepsilon_1 = 0.3919$  and  $\varepsilon_2 = 1$ . (a) Phase diagram  $x_1$  versus  $x_2$ . (b) Phase diagram  $x_1$  versus  $x_2$ . (c) Variation of electrical voltage.

Analyzing Figure 4, the chaotic behavior of the system is proven, for  $K \approx 0.9$ . However, Figure 5 shows a periodic behavior, which was to be expected, since  $K \approx 0$ .

In Figure 6, the variation of the average power of energy generation and the  $K$  parameter of test 0-1 are presented, considering variations of  $\varepsilon_1 = [0.01: 2]$  versus  $\rho = [0.01: 2]$ , with fixed value for  $\alpha_2 = 0.1$ .

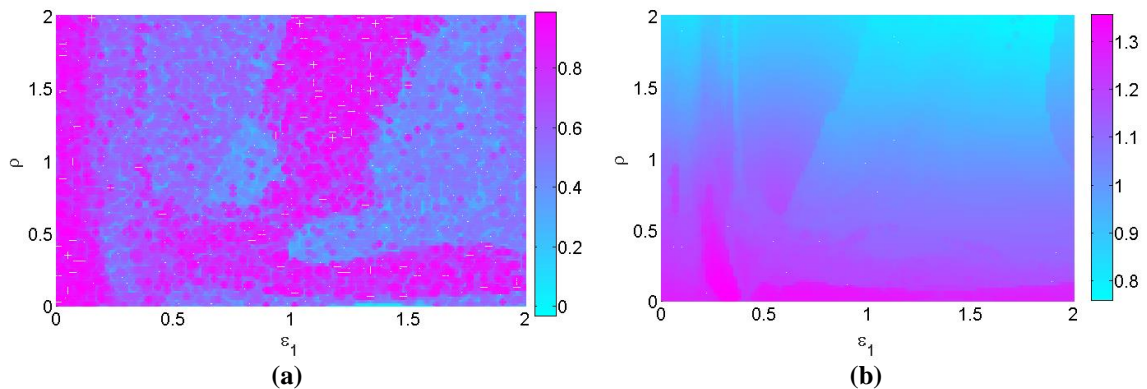


Figure 6. Variation in parameters  $\varepsilon_1 = [0.01: 2]$  versus  $\rho = [0.01: 2]$ . (a) Test 0-1. (b) Average Power.

Figure 6 shows that, for lower values of  $\rho$ , we have a more significant potential for energy generation, taking the system to defined regions with quasi-periodic behavior.

Thus, in case of  $\varepsilon_1 = 0.03316$  and  $\rho = 0.01$  an average power  $P_{avg} \approx 1.355$  is obtained, with  $K \approx 0.5$ , configuring the system with a quasi-periodic behavior, as it is neither completely periodic nor chaotic.

We can also observe that there is a region with chaotic behavior that also provides a good level of energy generation for values close to  $\varepsilon_1 = 0.0904$  and  $\rho = 0.0703$ . For these parameters, we obtain an average power of energy  $P_{avg} \approx 1.253$ , with  $K \approx 0.9$ .

Figure 7 shows the phase diagram of the gantry and the NES as well as the time history of the electrical voltage generated by the piezoelectric material for the parameters:  $\varepsilon_1 = 0.03316$  and  $\rho = 0.01$ . And in Figure 8 for parameters:  $\varepsilon_1 = 0.0904$  and  $\rho = 0.0703$ .

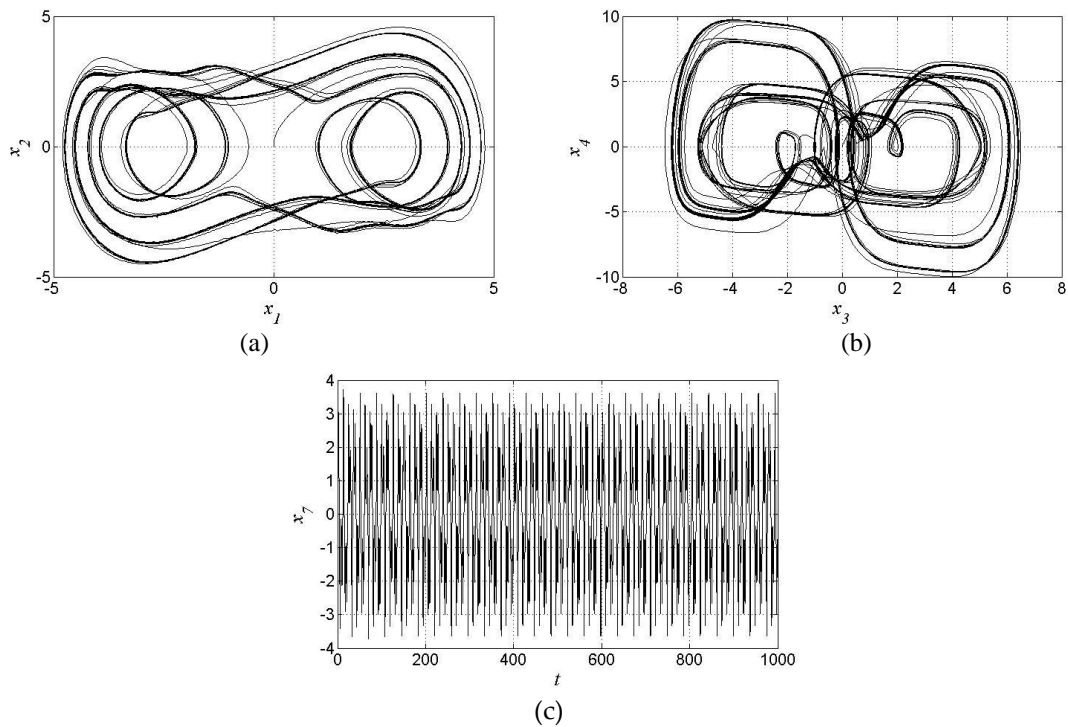


Figure 7. Case that  $\varepsilon_1 = 0.03316$  and  $\rho = 0.01$ . (a) Phase diagram  $x_1$  versus  $x_2$ . (b) Phase diagram  $x_1$  versus  $x_2$ . (c) Variation of electrical voltage.

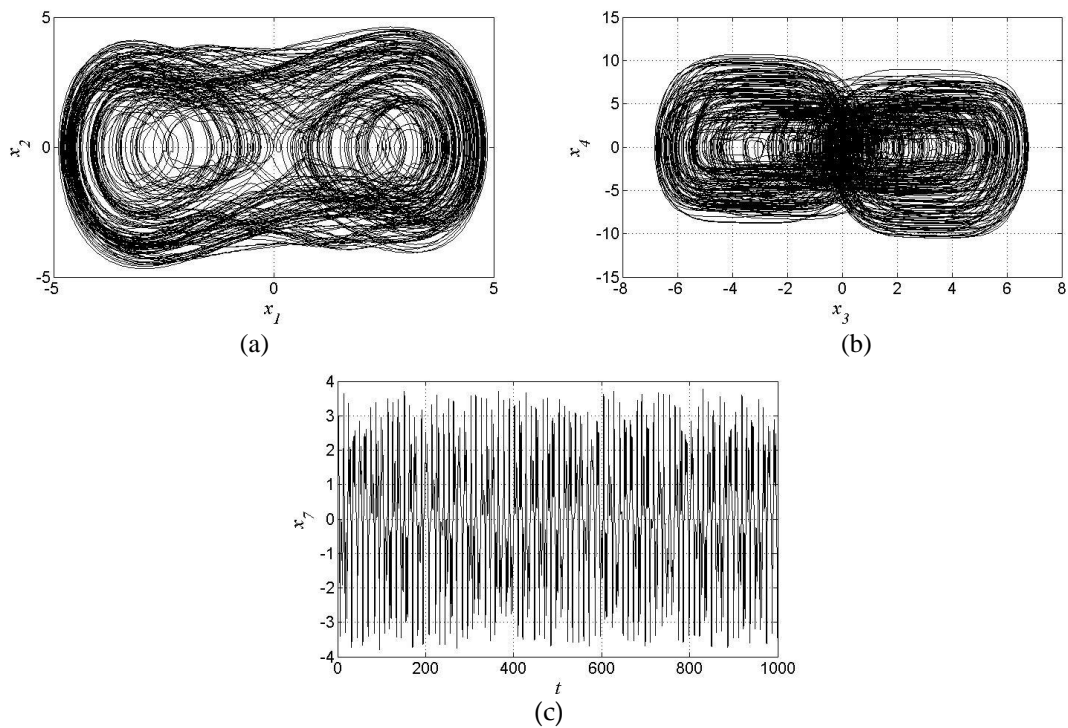


Figure 8. Case that  $\varepsilon_1 = 0.0904$  and  $\rho = 0.0703$ . (a) Phase diagram  $x_1$  versus  $x_2$ . (b) Phase diagram  $x_1$  versus  $x_2$ . (c) Variation of electrical voltage.

Analyzing the results of Figure 7 we see that the chaotic behavior is not evident, and neither is the periodic behavior, as  $K \approx 0.5$ , in this work, we will consider the behavior with quasi-periodic. However, the chaotic behavior is evident in Figure 8.

Figure 9 shows the dynamics of the system, and the potential for power generation, considering variations in the parameters  $\varepsilon_2 = [1: 10]$  and  $\rho = [0.01: 2]$  and fixed parameter  $\varepsilon_1 = 1$ .

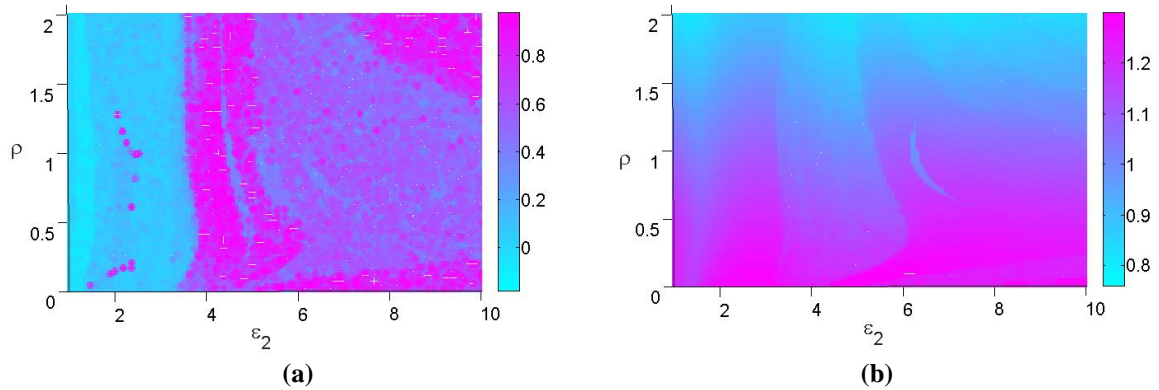


Figure 9. Variation in parameters  $\varepsilon_2 = [1: 10]$  versus  $\rho = [0.01: 2]$ . (a) Test 0-1. (b) Average Power.

Figure 9 shows that, as the value of  $\rho$  decreases, a higher energy generation value is obtained, leading the system to a quasi-periodic or periodic behavior. It was possible to get an average power energy of  $P_{avg} = 1.299$ , and  $K \approx 0.4$ , for the parameters:  $\varepsilon_2 = 4.909$  and  $\rho = 0.0301$ , and an average power of energy  $P_{avg} = 1.291$  and  $K \approx 0$ , for the parameters  $\varepsilon_2 = 6.636$  and  $\rho = 0.01$ .

Figure 10 shows the phase diagram of the gantry and the NES as well as the time history of the electrical voltage generated by the piezoelectric material for the parameters:  $\varepsilon_2 = 4.909$  and  $\rho = 0.0301$ . And in Figure 11 for parameters:  $\varepsilon_2 = 6.636$  and  $\rho = 0.01$ .

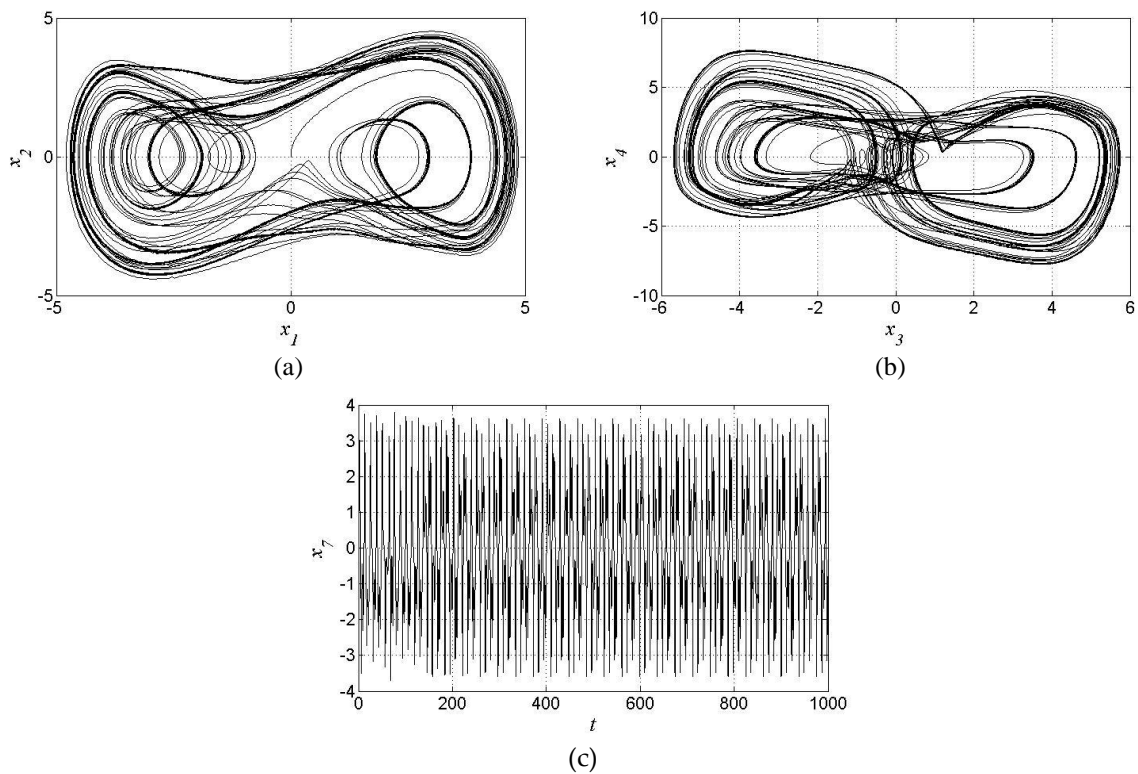


Figure 10. Case that  $\varepsilon_2 = 4.909$  and  $\rho = 0.0301$ . (a) Phase diagram  $x_1$  versus  $x_2$ . (b) Phase diagram  $x_1$  versus  $x_2$ . (c) Variation of electrical voltage.

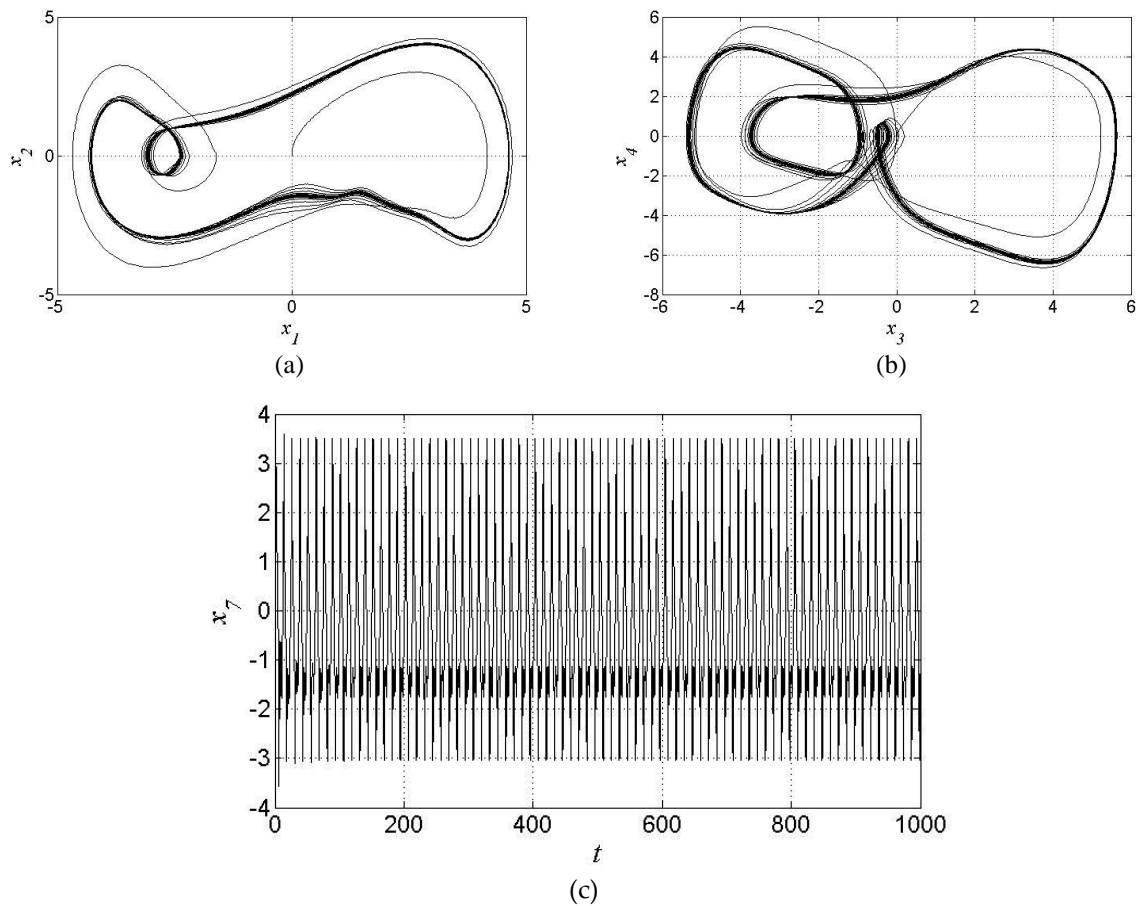


Figure 11. Case that  $\varepsilon_2 = 6.636$  and  $\rho = 0.01$ . (a) Phase diagram  $x_1$  versus  $x_2$ . (b) Phase diagram  $x_1$  versus  $x_2$ . (c) Variation of electrical voltage.

Analyzing the results of Figure 10 we see that the chaotic behavior is not evident, and neither is the periodic behavior, as  $K \approx 0.4$ , in this work, we will consider the behavior with quasi-periodic. However, the periodic behavior is evident in Figure 11.

#### 4. CONCLUSIONS

The presented results in the work demonstrate the significant influence of the piezoelectric material parameters on the system's dynamic behavior. Since the piezoelectric material can be used both as an actuator and sensor, its use as a source of energy is essential for green energy harvesting. The stored energy, in turn, can be used later in applying the piezoelectric material as an actuator.

With the 0-1 test, it was possible to verify which parameters can lead the system into chaotic behavior, which is not desired in most applications. The study also confirmed that the NES system is a good alternative for controlling vibrations without energy consumption.

#### 5. ACKNOWLEDGEMENTS

The first author thanks CNPq for the financial support (Process: 310562/2021-0). The second author thanks CNPq for the financial support (Process: 309799/2021-0).

#### 6. REFERENCES

- Aoudia, F.A., Gautier, M., Magno, M., Berder, O., Benini, L., 2018. "Leveraging Energy Harvesting and Wake-up Receivers for Long-Term Wireless Sensor Networks". *Sensors*, Vol. 18, p. 1578.
- Bao, B., Wang, Q., 2021. "A Rain Energy Harvester Using a Self-Release Tank". *Mech Syst Signal Process*, Vol. 147, p. 107099.
- Bernardini, D., Litak, G., 2016. "An Overview of 0–1 Test for Chaos". *Journal of the Brazilian Society of Mechanical Sciences and Engineering*, Vol. 38, p. 1433-1450.

- Cao, X., Xiong, Y., Sun, J., Zhu, X., Sun, Q., Wang, Z.L., 2021. "Piezoelectric Nanogenerators Derived Self-Powered Sensors for Multifunctional Applications and Artificial Intelligence". *Adv Funct Mater*, Vol. 31, p. 102983.
- Du, X., Mutsuda, H., Tanaka, Y., Nakashima, T., Kanehira, T., Taniguchi, N., Moriyama, Y., 2022. "Experimental and Numerical Studies on Working Parameter Selections of a Piezoelectric-Painted-Based Ocean Energy Harvester Attached to Fish Aggregating Devices". *Energy for Sustainable Development*, Vol. 71, p. 73–88.
- Eiras, J.A., Gerbasi, R.B.Z., Rosso, J.M., Silva, D.M., Cótica, L.F., Santos, I.A., Souza, C.A., Lente, M.H., 2016. "Compositional Design of Dielectric, Ferroelectric and Piezoelectric Properties of (K,Na)NbO<sub>3</sub> and (Ba, Na)(Ti, Nb)O<sub>3</sub> Based Ceramics Prepared by Different Sintering Routes". *Materials*, Vol. 9, p. 179.
- Elahi, H., Munir, K., Eugeni, M., Abrar, M., Khan, A., Arshad, A., Gaudenzi, P., 2020. "A Review on Applications of Piezoelectric Materials in Aerospace Industry". *Integrated Ferroelectrics*, 211, p. 25–44.
- Fang, L.H., Rahim, R.A., Fahmi, M.I., Kupusamy, V., 2023. "Modelling and Characterization Piezoelectric Transducer for Sound Wave Energy Harvesting". *Journal of Advanced Research in Fluid Mechanics and Thermal Sciences*, Vol. 102, p. 81–98.
- Gottwald, G.A., Melbourne, I., 2004. "A New Test for Chaos in Deterministic Systems. *Proceedings of the Royal Society A: Mathematical, Physical and Engineering Sciences*, Vol. 460, p. 603-611.
- Gottwald, G.A., Melbourne, I., 2005. "Testing for Chaos in Deterministic Systems with Noise". *Physica D*, Vol. 212, p. 100–110.
- Holzmann, H., Weber, M., Park, Y.J., Perfetto, S., Atzrodt, H., Dafnis, A., 2021. "Investigation of Biogenic Materials and Ferroelectrets for Energy Harvesting on Vibrating Aircraft Structures". *CEAS Aeronaut J*, Vol. 12, p. 331-344.
- Iliuk, I., Balthazar, J.M., Tusset, A.M., Piqueira, J., De Pontes, B.R., Felix, J., Bueno, A.M., 2014. "Application of Passive Control to Energy Harvester Efficiency Using a Non-ideal Portal Frame Structural Support System". *J Intell Mater Syst Struct*, Vol. 25, p. 417–429.
- Koga, H., Mitsuya, H., Honma, H., Fujita, H., Toshiyoshi, H., Hashiguchi, G., 2017. "Development of a Cantilever-Type Electrostatic Energy Harvester and Its Charging Characteristics on a Highway Viaduct". *Micromachines*, Vol. 8, p. 293.
- Lai, Y.C., Hsiao, Y.C., Wu, H.M., Wang, Z.L., 2019. "Waterproof Fabric-Based Multifunctional Triboelectric Nanogenerator for Universally Harvesting Energy from Raindrops, Wind, and Human Motions and as Self-Powered Sensors". *Advanced Science*, Vol. 6, p. 1801883.
- Litak, G., Bernardini, D., Syta, A., Rega, G., Rysak, A., 2013. "Analysis of Chaotic Non-Isothermal Solutions of Thermomechanical Shape Memory Oscillators". *European Physical Journal: Special Topics*, Vol. 222, p. 1637-1647.
- Lu, C., Jiang, X., Li, L., Zhou, H., Yang, A., Xin, M., Fu, G., Wang, X., 2022. "Wind Energy Harvester Using Piezoelectric Materials". *Review of Scientific Instruments*, vol. 93, p. 187-207.
- Mokhtari, F., Azimi, B., Salehi, M.; Hashemikia, S., Danti, S., 2021. "Recent Advances of Polymer-Based Piezoelectric Composites for Biomedical Applications". *J Mech Behav Biomed Mater*, Vol. 122, p. 104669.
- Pan, H., Qi, L., Zhang, Z., Yan, J., 2021. "Kinetic Energy Harvesting Technologies for Applications in Land Transportation: A Comprehensive Review". *Appl Energy*, Vol. 286, p. 116518.
- Panayanthatta, N., Clementi, G., Ouhabaz, M., Costanza, M., Margueron, S., Bartaszyte, A., Basrou, S., Bano, E., Montes, L., Dehollain, C., 2021. "A Self-Powered and Battery-Free Vibrational Energy to Time Converter for Wireless Vibration Monitoring". *Sensors*, Vol. 21, p. 7503.
- Ram, G.D., Kumar, S.P., Yuvaraj, T., Babu, T.S., Balasubramanian, K., 2022. "Simulation and Investigation of MEMS Bilayer Solar Energy Harvester for Smart Wireless Sensor Applications". *Sustainable Energy Technologies and Assessments*, Vol. 52, p. 102102.
- Selleri, G., Poli, F., Neri, R., Gasperini, L., Gualandi, C., Soavi, F., Fabiani, D., 2023. "Energy Harvesting and Storage with Ceramic Piezoelectric Transducers Coupled with an Ionic Liquid-Based Supercapacitor". *J Energy Storage*, Vol. 60, p. 106660.
- Shaukat, H., Ali, A., Bibi, S., Mehmood, S., Altabay, W.A., Noori, M., Kouritem, S.A., 2023. "Piezoelectric Materials: Advanced Applications in Electro-Chemical Processes". *Energy Reports*, Vol. 9, p. 4306–4324.
- Shi, S., Yue, Q., Zhang, Z., Yuan, J., Zhou, J., Zhang, X., Lu, S., Luo, X., Shi, C., Yu, H., 2018. "A Self-Powered Engine Health Monitoring System Based on L-Shaped Wideband Piezoelectric Energy Harvester". *Micromachines*, Vol. 9, p. 629.
- Tommasino, D., Moro, F., Zumalde, E., Kunzmann, J., Doria, A., 2023. "An Analytical–Numerical Method for Simulating the Performance of Piezoelectric Harvesters Mounted on Wing Slats". *Actuators*, Vol. 12, p. 29.
- Vallem, V., Sargolzaeiaval, Y., Ozturk, M., Lai, Y.C., Dickey, M.D., 2021. "Energy Harvesting and Storage with Soft and Stretchable Materials". *Advanced Materials*, Vol. 33, p. 2004832.
- Wu, M., Yao, K., Li, D., Huang, X., Liu, Y., Wang, L., Song, E., Yu, J., Yu, X., 2021. "Self-Powered Skin Electronics for Energy Harvesting and Healthcare Monitoring". *Mater Today Energy*, Vol. 21, p. 100786.
- Ye, J., Ding, G., Wu, X., Zhou, M., Wang, J., Chen, Y., Yu, Y., 2023. "Development and Performance Research of PSN-PZT Piezoelectric Ceramics Based on Road Vibration Energy Harvesting Technology". *Mater Today Commun*, Vol. 34, p. 105135.

## **7. RESPONSIBILITY NOTICE**

The authors are the only responsible for the printed material included in this paper.